TISSUE ENGINEERING: Part A
Volume 27, Numbers 15 and 16, 2021
© Mary Ann Liebert, Inc.
DOI: 10.1089/ten.tea.2020.0273

termis
Tissue Engineering
& Regenerative Medicine
International Society

ORIGINAL ARTICLE

Formation of Osteochondral Organoids from Murine Induced Pluripotent Stem Cells

Shannon K. O'Connor, MD, PhD,[1–3,*] Dakota B. Katz, BS,[1,2,4,5,*] Sara J. Oswald, MS,[1,2,5] Logan Groneck, BS,[1,2,4] and Farshid Guilak, PhD[1,2,4,5]

Osteoarthritis is a debilitating joint disease that is characterized by pathologic changes in both cartilage and bone, potentially involving cross talk between these tissues that is complicated by extraneous factors that are difficult to study *in vivo*. To create a model system of these cartilage–bone interactions, we developed an osteochondral organoid from murine induced pluripotent stem cells (iPSCs). Using this approach, we grew organoids from a single cell type through time-dependent sequential exposure of growth factors, namely transforming growth factor β-3 and bone morphogenic protein 2, to mirror bone development through endochondral ossification. The result is a cartilaginous region and a calcified bony region comprising an organoid with the potential for joint disease drug screening and investigation of genetic risk in a patient or disease-specific manner. Furthermore, we also investigated the possibility of the differentiated cells within the organoid to revert to a pluripotent state. It was found that while the cells themselves maintain the capacity for reinduction of pluripotency, encapsulation in the newly formed 3D matrix prevents this process from occurring, which could have implications for future clinical use of iPSCs.

Keywords: chondrogenic, osteogenic, iPSC, tissue engineering, organoid, scaffold-free, osteoarthritis

Impact Statement

The regeneration of integrated articular cartilage and bone tissues from a single cell source has been a challenge in the field of osteochondral tissue engineering and osteoarthritis disease modeling. The goal of this study was to develop an osteochondral organoid system using a single murine induced pluripotent stem cell (iPSC) source in a scaffold-free system and to determine whether differentiated iPSCs retain the potential to undergo reinduction of pluripotency. Our findings indicate that sequential differentiation into chondrogenic and osteogenic lineages can be used to develop osteochondral organoids, and encapsulation within a cartilaginous matrix prevents the reinduction of pluripotency in differentiated iPSCs.

Introduction

Osteoarthritis (OA) is a whole joint disease characterized by the degradation of articular cartilage with changes also occurring in the subchondral bone, including osteophyte formation and increased bone remodeling.[1–3] *In vitro* systems consisting of chondrocytes or tissue explants provide important model systems for studying cartilage biology and often serve as the initial basis for screening of disease-modifying OA drugs (DMOADs). However, the joint is increasingly viewed as a complex organ, with diseases impacting multiple tissues on many levels. To focus on the cross talk between cartilage and bone, the development of a model system that consists of these two tissues could provide additional insight into osteochondral biology and drug development.[2,4–6] In this regard, ''organoids'' are an emerging field that could present a platform for studying interactions of multiple tissues *in vitro*, as well as being a model for testing of DMOADs.[7–10]

Several tissue engineering approaches have been developed for the creation of an osteochondral construct that is designed for implantation as a means of replacing or repairing injured or diseased tissues in the joint.[7,11] The strategies used for creating these constructs generally rely on the use of a variety

[1]Department of Orthopaedic Surgery, Washington University in St. Louis, St. Louis, Missouri, USA.
[2]Shriners Hospitals for Children, St. Louis, St. Louis, Missouri, USA.
[3]Department of Biomedical Engineering, Duke University, Durham, North Carolina, USA.
[4]Department of Biomedical Engineering and [5]Center of Regenerative Medicine, Washington University, St. Louis, Missouri, USA.
*These authors contributed equally to this work.

of cell sources, scaffold materials, or geometries to create a bilayer or gradient from cartilage to bone or bioreactors to spatially deliver different media and growth factors to create the different tissues.[7,11–14] Instead, as a construct design strategy, bone development can be taken into consideration: long bones are formed when cartilage anlagen are subsequently converted to bone through endochondral ossification.[15] The cells that contribute to this osseous tissue formation may be either osteogenic cells that replace the hypertrophic chondrogenic cells or chondrocyte-like cells that transdifferentiate directly to osteogenic cells.[16–18] Indeed, several tissue engineering approaches have attempted to enhance osteogenesis of mesenchymal stem cells (MSCs) by differentiating them through an initial chondrogenic precursor phase.[19,20]

Induced pluripotent stem cells (iPSCs) provide a highly expandable and genetically-defined source of pluripotent cells for organoid tissue engineering: they exhibit pluripotency, allowing for multiple tissue types to be differentiated from a single cell source.[21] In addition, iPSCs are a powerful tool for investigation of genetic diseases, as they can be reprogrammed from the tissue of a patient with that disease[22] or genetically modified using genome-editing methods to develop disease-specific organoid models.[23] Subsequently, drug screening can be accomplished in a patient or disease-specific manner.[24]

In osteochondral tissue engineering, previous work has determined differentiation protocols of murine iPSCs (miPSCs) to both chondrogenic and osteogenic lineages individually, utilizing transforming growth factor β (TGF-β) and bone morphogenic protein 2 (BMP2) to drive the specific differentiation.[25,26] Additional previous work has demonstrated bone-like and cartilage-like composites from miPSCs.[27] However, recapitulation of endochondral ossification in miPSCs to create an osteochondral organoid has not previously been done. By synthesis of these separate differentiation protocols, iPSCs enable investigation not only of the endochondral ossification pathway but also the potential for transdifferentiation of chondrocytes in the development of osseous tissue.

This study demonstrates a time-dependent method for the creation of tissue-engineered osteochondral organoids for use in osteochondral research as a step toward future clinical applications. To create an osteochondral organoid, we differentiated iPSCs down a chondrogenic lineage using TGF-β3 and subsequently induced osseous tissue formation by utilizing BMP2. We characterized this osteochondral organoid to verify both chondrogenesis and osteogenesis. We also examined the hypothesis that re-exposure of the cells to the Yamanaka factors used to initially induce pluripotency in the mouse tail fibroblast (*Oct4*, *Sox2*, *Klf4*, and *cMyc*) would revert the cells back to a pluripotent state following terminal chondrogenic differentiation.[28] This would allow for subsequent differentiation to a different cell lineage.

The iPSCs used in this study were initially induced using a doxycycline-inducible lentiviral vector for the pluripotency factors. Therefore, it was hypothesized that adding doxycycline to the culture media would reactivate this vector and result in expression of the Yamanaka factors. This approach would allow us to test whether reinduction of pluripotency in chondrogenically-differentiated cells would facilitate the sequential induction of osteogenesis, in comparison to osteogenic induction through direct transdifferentiation of the chondrocyte-like cells to osteogenic cells. In addition, further elucidation of the functionality of the doxycycline-inducible vector on terminally-differentiated cells is vital for the safety of future iPSC-derived engineered constructs for clinical applications.[29–31]

Method

Prechondrogenic differentiation and sorting of miPSCs

The timeline for experimental methods is shown in Figure 1. miPSCs were induced, cultured, and sorted for chondrogenic potential as previously described.[25] Briefly, a previously-derived iPSC line was created from mouse tail fibroblasts that were transduced with a doxycycline-inducible lentiviral vector for the expression of Sox2, Oct4 (pou5f1), Klf4, and c-Myc and cultured in iPSC media containing

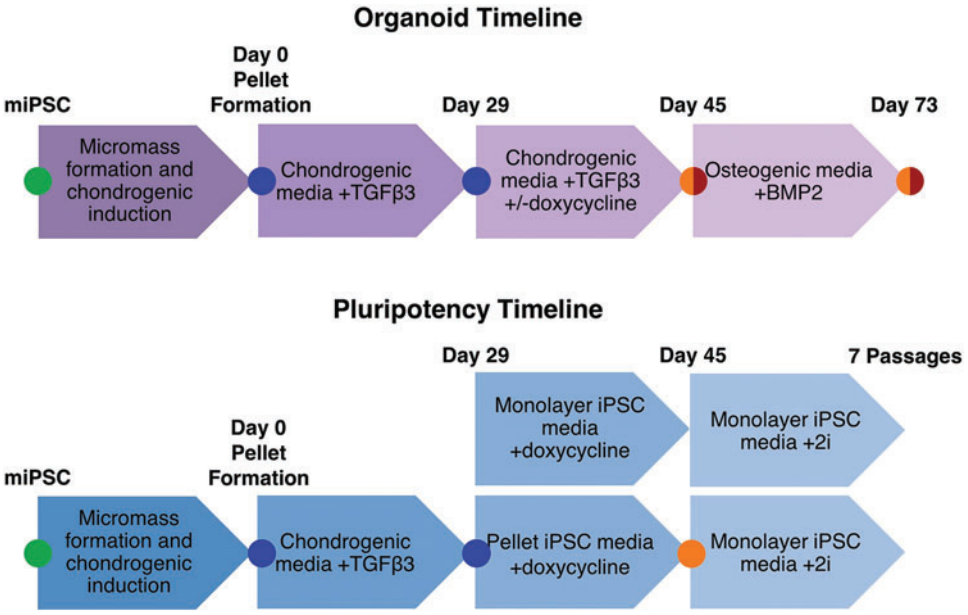

FIG. 1. Timelines for organoid formation and pluripotency testing. Data collection points shown for miPSCs (*green*), pellets in chondrogenesis (*blue*), and samples with or without doxycycline (dox) treatment (*yellow*/*red*). iPSC, induced pluripotent stem cell; miPSC, murine iPSC. Color images are available online.

dulbecco's modified eagle's medium - high glucose (DMEM-HG) (Gibco), 20% lot-selected fetal bovine serum (FBS; Atlanta Biologicals), MEM nonessential amino acids (NEAA; Gibco), β-mercaptoethanol (Gibco), gentamicin (Gibco), and mouse leukemia inhibitory factor (LIF; Millipore ESGRO). miPSCs were nucleofected with a linearized pCOL2-EGFP-SV40-NEO reporter plasmid (kindly provided by Dr. William Horton, Shriners Hospitals for Children - Portland).[32] Cells were then expanded between days 2 and 12 post-transfection with G418 (200 μg/mL; Invitrogen) as previously described.[25] G418-resistant clones were individually expanded and differentiated in micromass culture in chondrogenic media containing DMEM-HG (Gibco), NEAA (Gibco), β-mercaptoethanol (Gibco), ITS+ (BD), penicillin–streptomycin (Gibco), 50 μg/mL L-ascorbic acid 2-phosphate (Sigma), and 40 μg/mL L-proline (Sigma). Micromasses were treated with 50 ng/mL mBMP-4 (R&D Systems) and 100 nM dexamethasone on days 3–5 of culture.

Post micromass culture, the micromasses were digested for 1 h at 37°C using 0.4% collagenase type II (Worthington), 1320 PKU/mL pronase (Calbiochem), and 10 μg/mL DNase I (Worthington) and pipetted every 15 min during incubation. Cells were centrifuged, incubated with 0.25% trypsin-ethylenediaminetetraacetic acid (EDTA) for 5 min, and resuspended in sort medium containing DMEM-HG, 2% FBS, DNase I, 10 mM Hepes (Gibco), 2× penicillin-streptomycin-fungizone, and 5 μM propidium iodide (BioLegend). Cells were sorted based on GFP expression using the 100 μM nozzle of an Aria II flow sorter (BD BioSciences). Approximately 10–20% of cells were GFP+ and therefore collagen II positive.

Pellet culture for chondrogenesis, osteogenesis, and pluripotency reinduction

After sorting, cells were expanded on gelatin-coated plates at 1×10^4 cells/cm^2 in chondrogenic differentiation media with 4 ng/mL human basic fibroblast growth factor (hbFGF) (Roche) and 10% FBS. Cells were passaged every 3 days for two passages using 0.05% trypsin-EDTA for 5 min. After the second passage, cells were resuspended in chondrogenic media with 10 ng/mL TGF-β3 and pelleted by centrifugation at 2.5×10^5 cells/pellet, 200 *g* for 5 min in 15 mL conical tubes.

Pellets were cultured in chondrogenic media for 29 days, with media changes every 3 days. For osteochondral organoids, pellets continued to be cultured with 10 ng/mL TGF-β3 in chondrogenic media for 16 additional days with or without the addition of 10 μg/mL doxycycline (Sigma) followed by 28 days in osteogenic media containing 12.5 ng/mL BMP2 (RnD), 10% FBS, DMEM-HG (Gibco), NEAA (Gibco), β-mercaptoethanol (Gibco), penicillin-streptomycin (Gibco), 50 μg/mL L-ascorbic acid 2-phosphate (Sigma), dexamethasone, and 10 mM β-glycerophosphate (Sigma).

Mycoplasma testing was performed regularly by a core facility at Washington University. Additional DAPI staining further demonstrated negative mycoplasma results.

Gene expression by qRT-PCR

Pellets were homogenized in lysis buffer in a bead beater. RNA isolation was performed according to manufacturer's instructions (Total RNA Purification Plus Micro Kit, Norgen). cDNA synthesis was performed using SuperScript IV First-Strand Synthesis System (Thermo Fisher), in parallel with a No Template Control (NTC). PCR was performed with TaqMan Gene Expression Assay probes (Thermo Fisher) (Table 1) and TaqMan Fast Advanced Master Mix. Data analysis was performed with the ΔΔCT method. GAPDH was used as the endogenous control gene. All samples were compared to miPSCs.

Histology and immunohistochemistry

Pellets were fixed in 10% Neutral Buffered Formalin for 16 h and dehydrated, paraffin embedded, and sectioned at 8 μm thickness. Safranin-O/fast green/hematoxylin staining was performed under standard protocols using osteochondral sections from mouse knee joints as controls. Von Kossa staining was performed according to manufacturer's instructions (Abcam), with a knee joint dissected from an 11-day-old mouse as control.

For immunohistochemistry, sections were treated with xylene and ethanol in decreasing concentrations. For type II collagen (Iowa II-II6B3, 1:1 in 10% goat serum), type VI collagen (Fitzgerald 70R-CR009×, 1:1000 in 1% BSA), and type X collagen (Sigma c7974, 1:400), epitope retrieval was performed with Digest-All 3 Pepsin (Invitrogen) at room temperature for 5 min, treated with a methanol-peroxidase solution, blocked for 30 min (goat serum for type X collagen, goat serum with the addition of cold fish gelatin for type II collagen, and for type VI collagen, 2% goat serum, 1% BSA, 0.1% Triton X-100, 0.05% Tween 20, 0.01 M PBS (pH 7.2)), then incubated for an hour at room temperature in primary antibody. Secondary antibody incubation was performed for 30 min at room temperature (ab97021 for type II collagen and type X collagen and ab6720 for type VI collagen, 1:500), followed by HRP Streptavidin treatment and

Table 1. Quantitative Polymerase Chain Reaction Primer Probes

Gene	*Name*	*Probe*
Acan	Aggrecan	Mm00545794_m1
Alpl	Alkaline phosphatase	Mm00475834_m1
Bglap	Osteocalcin	Mm03413826_mH
Col1a2	Type I collagen	Mm00483888_m1
Col2a1	Type II collagen	Mm01309565_m1
Col10a1	Type 10 collagen	Mm00487041_m1
Gapdh	Glyceraldehyde 3-phosphate dehydrogenase	Mm99999915_g1
Hprt	hypoxanthine guanine phosphoribosyl transferase	Mm00446968_m1
Ibsp	Bone sialoprotein	Mm00492555_m1
Nanog	Nanog homeobox	Mm01617762_g1
Oct4/Pou5F1	Octamer-binding transcription factor 4	Mm03053917_g1
Prg4	Lubricin	Mm01284582_m1
Runx2	Runt-related transcription factor 2	Mm00501584_m1
Sox2	sex determining region Y-box 2	Mm03053810_s1
Sox9	sex determining region Y-box 9	Mm00448840_m1
Sp7	Osterix	Mm04209856_m1

AEC Red Single (Histostain Plus; Invitrogen), counterstained with hematoxylin, and mounted with VectaMount (Vector Labs). For type I collagen (8D4A1, Chondrex, 1:200, biotinylated), epitope retrieval was performed with proteinase K diluted in TE buffer and incubated at 37°C for 20 min, then treated with methanol-peroxidase solution, and blocked for 30 min (goat serum) before primary incubation. Type I collagen slides were not counterstained. Osteochondral sections from mouse knee joints were used as controls. Final histology images were taken on a VS120 microscope imaging system (Olympus) at 20× magnification, with consistent brightfield settings for each stain.

MicroCT analysis

Pellets were serially dehydrated to 70% ethanol for microCT imaging (SkyScan1176; Bruker) at 40 kV and 600 μA with no filter at a resolution of 8.75 μm. Images were reconstructed at dynamic range 0 to 0.16, beam hardening 20, ring artifact correction 10. Total pellet tissue volume (TV), calcified bone volume (BV), and bone mineral density (BMD) values were calculated based on comparison to hydroxyapatite phantoms using CTAnalyser software (Bruker). Images were generated in CTVox software (Bruker).

Biochemical analysis

Pellets were digested in papain at 65°C for 16 h. dsDNA was measured with PicoGreen dsDNA Quantitation Kit (Invitrogen), sulfated glycosaminoglycans (s-GAGs) were measured with the DMMB assay, and total collagen was measured with the hydroxyproline assay. To quantify calcium content, pellets were decalcified by incubating in 5% formic acid for 30 min. Calcium concentration was measured using the Calcium Colorimetric Assay Kit (Fisher).

Pluripotency testing

To test pluripotent potential, pellets were cultured up to day 29 as described above and then divided into two groups (Fig. 1). One group of pellets was cultured for 16 days in iPSC media containing 20% FBS, DMEM-HG (Gibco), NEAA (Gibco), β-mercaptoethanol (Gibco), gentamicin (Gibco), and mouse LIF (EMD Millipore), with 10 μg/mL doxycycline. The other group of pellets was dissociated using 0.4% collagenase type II (Worthington), 1320 PKU/mL pronase (Calbiochem), and 10 μg/mL DNase I (Worthington) and plated in monolayer on laminin-coated (Sigma L2020) plates in iPSC media with 10 μg/mL doxycycline, 1 μM PD0325901 (Cayman Chemical), and 3 μM CHIR99021 (Cayman Chemical) for feeder-free culture utilizing the 2i system for 16 days. The 2i-laminin system is used in place of using a feeder layer of cells to support pluripotency. It has been well established in the stem cell literature that this system does not induce pluripotency, but rather helps prevent differentiation in pluripotent cells. The maintenance of pluripotency by the laminin-2i system has been shown to last for eight passages.[33–35] After 16 days, the remaining pellets were also dissociated and plated in monolayer. Both monolayer iPSC groups were passaged seven additional times in iPSC media without doxycycline before staining for pluripotency markers.[33]

For imaging, 5×10^4 cells were plated into each well of a four-well chambered culture slide (Falcon/Corning) precoated with laminin. After culturing for 5 days, wells were rinsed 3× in phosphate-buffered saline (PBS), fixed in 4% paraformaldehyde in PBS with 0.1% Tween for 20 min at room temperature, rinsed 3× in PBS, permeabilized for 20 min at room temperature in 0.1% Triton X-100 in PBS, rinsed 4× in PBS with 0.1% Triton-X, and incubated in Blocking Buffer (10% FCS in PBS) for 40 min at room temperature. Primary antibodies were incubated overnight at 4°C in precooled Blocking Buffer (Abcam 1:100 for each: Nanog 80892, Oct4 27985, SSEA-1 16285). Wells were rinsed 4× in PBS with 0.1% Triton-X. Secondary antibodies were incubated for 75 min at 4°C in the dark in Blocking Buffer (all Invitrogen, for Nanog, 1:1000 Alexa Fluor Plus 488 (GFP) A-32731, for Oct4, 1:600 Alexa Fluor 568 (RFP) A-11057, and for SSEA-1, 1:1000, Alexa Fluor 647 (Cy5) A-32728). Wells were rinsed 2× in PBS with 0.1% Triton-X and mounted in Prolong Gold with DAPI (Invitrogen). Slides were imaged at 10× and 40× using the Cytation 5 system (Agilent Technologies).

Statistical analysis

Experimental data reported as mean ± SEM were compared using a Student's *t*-test, a one-way ANOVA followed by a *post hoc* Tukey's test, or a two-way ANOVA. Data were analyzed with JMP statistical software with a significance level set to $\alpha = 0.05$.

Experiment

Chondrogenic outcomes

After 15, 29, and 45 days of chondrogenic culture, expression of chondrogenic genes *Acan*, *Col2a1, Prg4,* and *Sox9* was significantly upregulated compared to original miPSCs or day 0 pellets (Fig. 2A). Chondrogenic gene expression decreased during the osteogenic phase from day 45 through day 73 but maintained expression levels significantly above miPSC levels. Doxycycline treatment had no statistically significant effect on gene expression at either day 45 or day 73.

DNA content in the pellets increased from day 45 to day 73 (Fig. 2B). Doxycycline treatment also increased DNA content compared to no treatment. Sulfated GAG content decreased after osteogenesis independent of doxycycline treatment. Total collagen between pre- and postosteogenesis groups was maintained, independent of doxycycline treatment.

Pellets cultured under chondrogenic conditions showed rich Safranin-O staining throughout the specimens at 45 days of culture (Fig. 2C). Collagen type II and type VI were confirmed to be present throughout the pellet by immunohistochemistry (IHC), while collagen type X was minimally present. No differences were noted between pellets with or without doxycycline treatment. Following osteogenic induction at day 73, s-GAGs, collagen type II, and collagen type VI were maintained in the pellet extracellular matrix (ECM) inside the constructs, with new tissue growth on the outside less rich in s-GAGs and collagen type II. This new tissue growth was rich in type VI collagen. Collagen type X was minimally present. These chondrogenic ECM components were present independent of treatment with doxycycline.

Osteogenic outcomes

After osteogenic induction, gene expression of *Alpl*, *Bglap*, *Col1a2, Ibsp, Runx2*, and *Sp7* were all significantly increased compared to miPSC levels (Fig. 3A). *Col10a1*, a

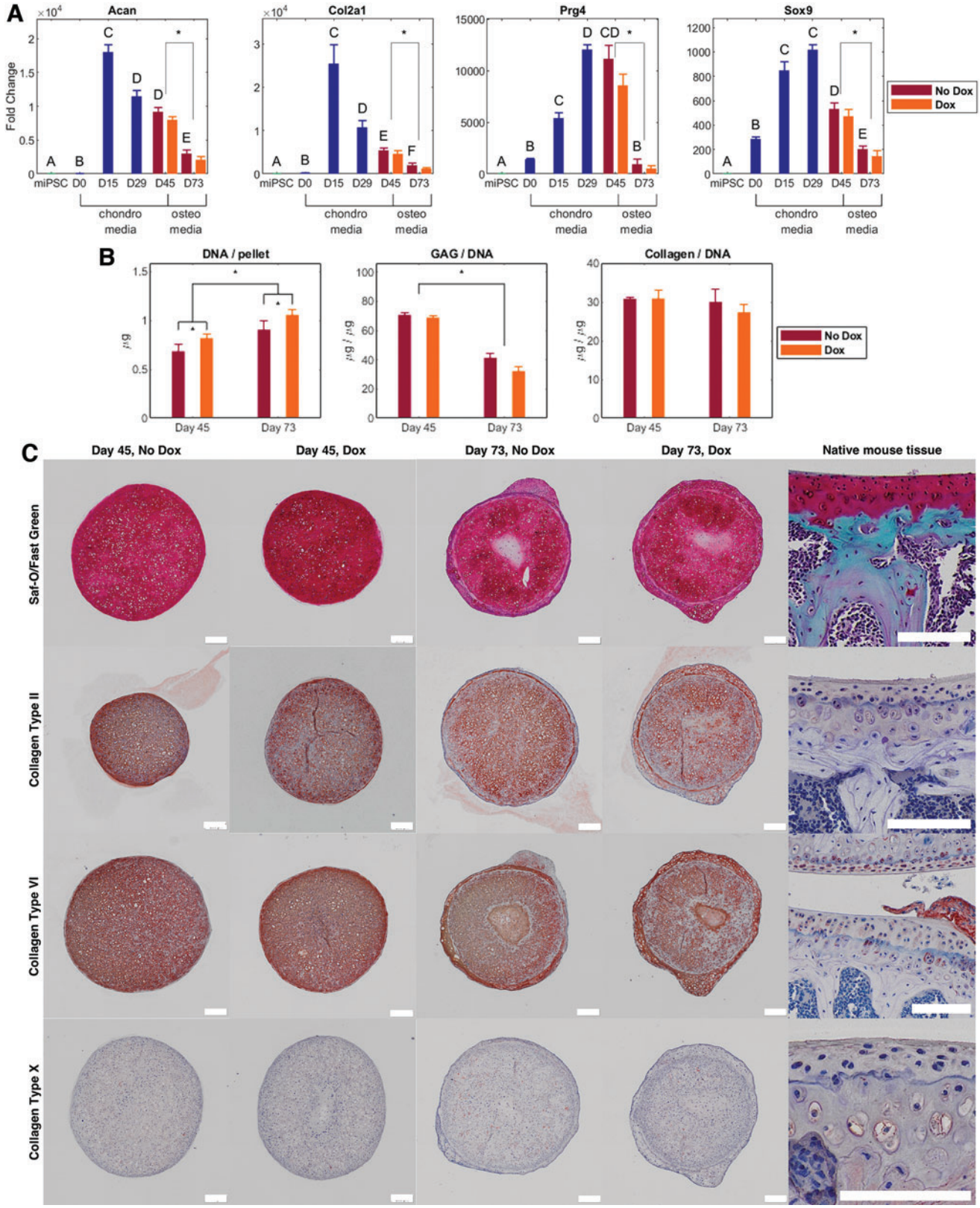

FIG. 2. Organoid chondrogenesis. **(A)** Gene expression of chondrogenic genes at days 0, 15, 29, 45, and 73 of culture compared to miPSCs. Reference gene is GAPDH. Data points and error bars demonstrate mean ± SEM. Groups not labeled with the same letter are significantly different by one-way ANOVA with *post hoc* Tukey–Kramer analysis with $p < 0.05$ (nondox groups only). Significance of two-way ANOVA for days 45 and 73 with and without dox denoted by *brackets* and *asterisks*. $n = 3$ for miPSC control, $n = 6$–8 for experimental groups. **(B)** Biochemical analysis of DNA and ECM components of pellets at days 45 and 73 with and without doxycycline treatment. Data points and error bars demonstrate mean ± SEM. Significance determined by two-way ANOVA with $p < 0.05$. Significance denoted by *brackets* and *asterisks*. $n = 4$. **(C)** Histologic analysis of pellets at days 45 and 73, with or without doxycycline treatment. *Top* to *bottom*: Safranin-O/fast *green*/hematoxylin staining, immunohistochemical probing of collagen type II, VI, and X (with mouse joint controls). Scale bars: 200 μm in pellet samples, 100 μm in mouse tissue controls. ECM, extracellular matrix. Color images are available online.

hypertrophy gene, was found to be highest at day 45, the end of the chondrogenic phase, and declined during the osteogenic phase. Doxycycline treatment had no statistically significant effect on gene expression.

Histologic analysis of organoids after a total of 73 days of culture showed osteogenic tissue formation in the outer region of the organoids, which were rich in collagen and mineralized tissue, as evidenced by IHC for collagen type I, Von Kossa staining, and Masson's Trichrome staining (Fig. 3B). MicroCT analysis of organoids at day 73 further confirmed the presence of a dense outer calcified region (Fig. 3C). Quantitative analysis of microCT images revealed similar BMD, BV, and the ratio of calcified bone volume to total tissue volume (BV/TV) between pellets with or without doxycycline treatment, although there was an increase in total TV in the constructs treated with doxycycline (Fig. 3D). A calcium assay of these organoids showed no calcification after the chondrogenic growth phase at day 45. After osteogenic induction, calcium per pellet increased to about 35 μg independent of prior doxycycline treatment (Fig. 3E).

Reinduction of pluripotency

To confirm the reactivation potential of the doxycycline-inducible lentiviral vector to express the Yamanaka factors and induce pluripotency, doxycycline was administered again after chondrogenesis to cultures either in monolayer or in pellet form. After doxycycline withdrawal, these cultures were maintained in a 2i-laminin system for seven passages before performing colony pluripotency assays. Cells were treated with doxycycline in monolayer formed colonies and showed positive staining for alkaline phosphatase, Nanog, Oct4, and SSEA-1, consistent with a pluripotent phenotype (Fig. 4A). However, cells from pellets exposed to doxycycline did not form colonies nor demonstrate expression of Nanog, Oct4, or SSEA-1. Some of these cells did stain positive for alkaline phosphatase, but the morphology of these cells was inconsistent with pluripotent stem cells.

Gene expression was assessed on days 0, 15, and 29 of chondrogenic culture and on day 45 after 16 days of doxycycline treatment in iPSC media: all groups demonstrated significantly lower levels of expression of *Alpl, Nanog, Oct4,* and *Sox2* compared to the miPSCs (Fig. 4B). *Alpl*, a complicated gene expressed not only in a pluripotent state but also in multiple other tissue types did increase after doxycycline exposure, but remained significantly lower than the miPSC group.

Together, these results demonstrate the potential for reactivation of the Yamanaka factors and de-differentiation to pluripotency in these cells after monolayer induction, but a resistance to de-differentiation within chondrogenic tissue.

Discussion

We have developed a scaffold and bioreactor-free method of creating osteochondral organoids *in vitro* through sequential exposure of iPSCs to chondrogenic and osteogenic growth factors, mimicking the process of endochondral ossification. Endochondral ossification has been studied for decades but remains incompletely understood. There are two main theories thought to govern this process: (1) chondrocytes create an articular cartilage matrix, calcify, die, and are replaced by new cells that migrate in from bone marrow that become osteocytes to complete the process of bone formation or (2) mature chondrocytes directly differentiate into osteocytes and osteoblasts to form bone tissue. There are many publications supporting both theories[15–18]; our findings support the latter theory, as there is no source of exogenous cells to repopulate the cartilaginous matrix.

Gene expression, histology, biochemical, and microCT analysis characterized the chondrogenic and osteogenic aspects of our osteochondral constructs. Given their pluripotent capabilities, as well as the ability to re-express the Yamanaka factors following differentiation, iPSCs also provide a defined system that allows us to examine their potential to revert once again to a pluripotent state after differentiation. Surprisingly, however, we found that chondrogenically differentiated cells within a cartilage pellet did not revert to a pluripotent state upon reinduction of the doxycycline-inducible pluripotency vector, although this vector was found to be both functional and capable of inducing pluripotency in cells isolated from pellets and grown in monolayer.

Previous *in vitro* osteochondral systems generally have utilized either terminally differentiated adult osteoblasts and chondrocytes or adult stem cells such as MSCs, to create the different tissue types necessary for organoid creation.[13,36–39] The utility of these terminally differentiated cells is limited by the relatively low number of cells that are able to be harvested. In addition, to create osteochondral organoids in a patient-specific manner, donor-site morbidity is an unwelcome side effect of cell harvest.[40] Furthermore, collection from diseased joints may further limit *in vitro* tissue synthesis in this manner. In contrast, iPSCs can be patient specific, readily expanded in culture while retaining their potential for differentiation, and harvested from a healthy tissue source.

Throughout 45 days of chondrogenic pellet culture, we found that gene expression for chondrogenic markers *Acan*, *Col2a1, Prg4,* and *Sox9* was upregulated over time. These

FIG. 3. Organoid osteogenesis. **(A)** Gene expression of osteogenic and hypertrophic genes at days 0, 15, 29, 45, and 73 of culture compared to miPSCs. Reference gene is GAPDH. Data points and error bars demonstrate mean ± SEM. Groups not labeled with the same letter are significantly different by one-way ANOVA with *post hoc* Tukey–Kramer analysis with $p < 0.05$ (nondox groups only). Significance of two-way ANOVA for days 45 and 73 with and without dox denoted by *brackets* and *asterisks*. $n = 3$ for miPSC control, $n = 6–8$ for experimental groups. **(B)** Histologic analysis of pellets at day 73 with and without doxycycline treatment. *Top* to *bottom*: Immunohistochemical probing of osteogenic protein collagen type I (with native mouse tendon control), Von Kossa staining (with nondecalcified young mouse knee control), and Masson's Trichrome staining (with adult mouse shoulder joint control). Scale bars: 200 μm in pellet samples, 100 μm in mouse tissue controls. **(C)** MicroCT images of pellets at day 73 with and without doxycycline treatment. Scale bars: 100 μm. **(D)** Quantification of MicroCT data for day 73 pellets with and without doxycycline treatment: BMD, calculated bone volume, total pellet tissue volume, and ratio of BV/TV. Significance of Student's *t*-test, $p < 0.05$, denoted by *brackets* and *asterisks*. $n = 4$. **(E)** Calcium content of pellet groups with and without doxycycline treatment at days 45 and 73. Data points and error bars demonstrate mean ± SEM. Significance of two-way ANOVA, $p < 0.05$, denoted by *brackets* and *asterisks*. $n = 4$. BMD, bone mineral density; BV/TV, bone volume to tissue volume. Color images are available online.

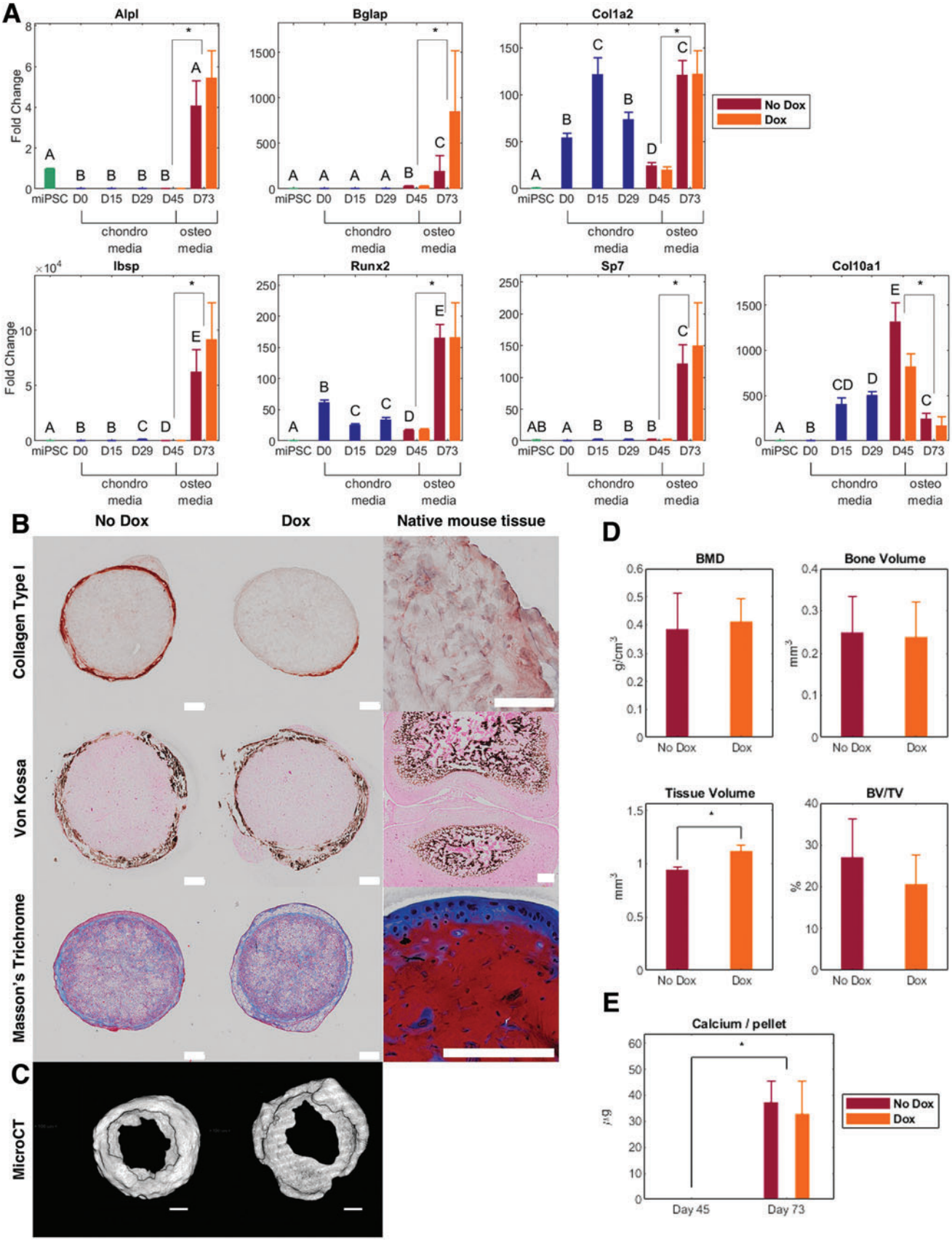
A
Alpl
Bglap
Col1a2
Ibsp
Runx2
Sp7
Col10a1
Fold Change
miPSC D0 D15 D29 D45 D73
chondro media
osteo media
No Dox
Dox
B
No Dox
Dox
Native mouse tissue
Collagen Type I
Von Kossa
Masson's Trichrome
C
MicroCT
D
BMD
Bone Volume
Tissue Volume
BV/TV
g/cm3
mm3
%
E
Calcium / pellet
Day 45
Day 73

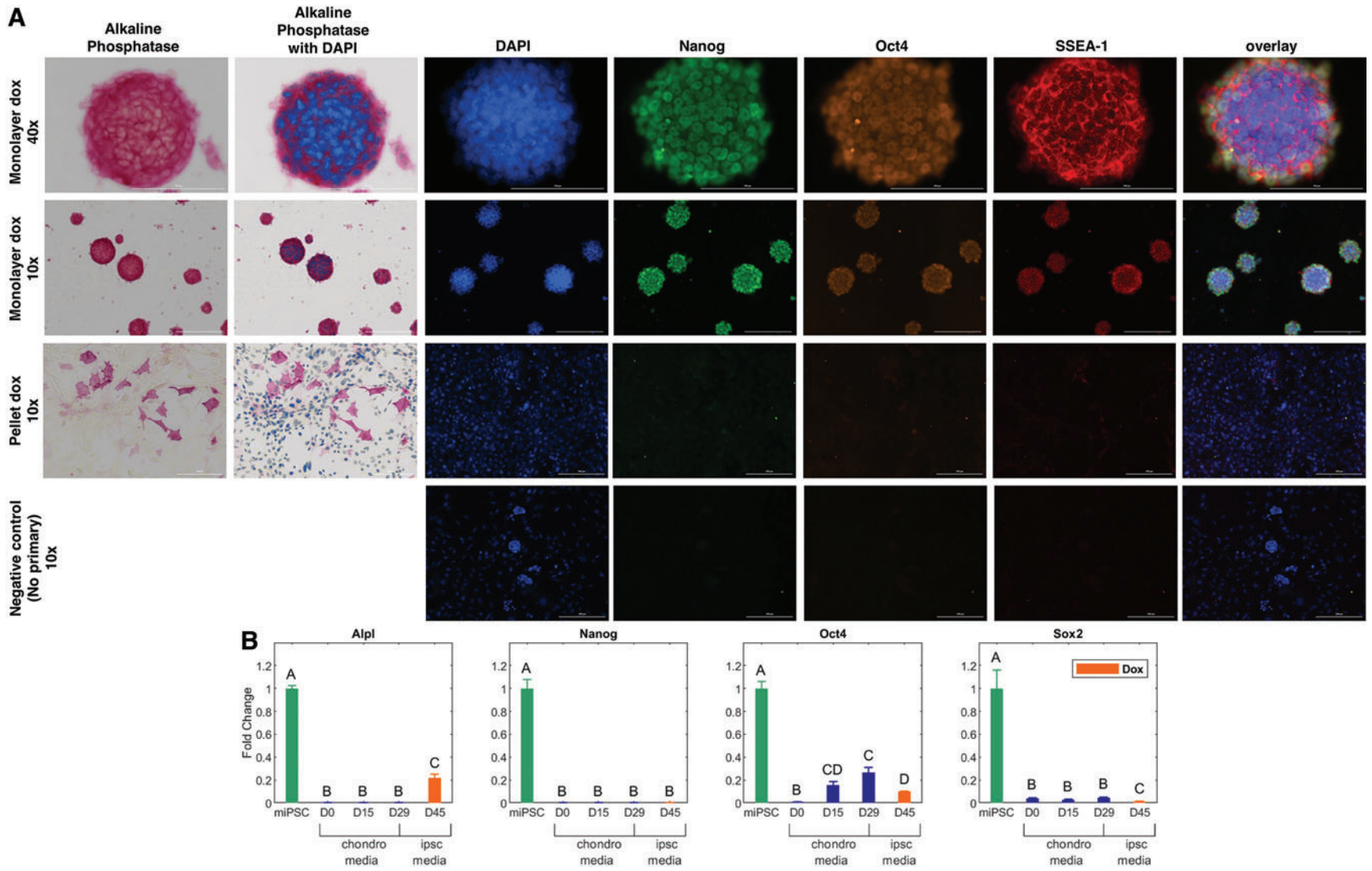

FIG. 4. Pluripotency outcomes. **(A)** Colony pluripotency assay. Groups from *top* to *bottom*: 40× images of doxycycline treatment in monolayer group, 10× images of doxycycline treatment in monolayer group, 10× images of doxycycline treatment in pellet group, 10× images of no primary antibody control. Positive alkaline phosphatase staining shown in *red*, with DAPI overlay in next *column*. Immunocytochemistry completed with fluorescent probes. Scale bars: 100 μm in 40× images, 200 μm in 10× images. **(B)** mRNA expression (qRT-PCR) of pluripotency genes at days 0, 15, and 29 of chondrogenic induction, as well as day 45 after replacing chondrogenic media with iPSC media with doxycycline. Control is initial miPSCs, and reference gene is GAPDH. Data points and error bars demonstrate mean ± SEM. Groups not labeled with the same letter are significantly different by one-way ANOVA with *post hoc* Tukey–Kramer analysis with $p < 0.05$. $n = 3$ for miPSC control, $n = 6$–8 for experimental groups. Color images are available online.

constructs showed a robust cartilaginous matrix with strong staining for s-GAGs and collagens type II and type VI and little staining for collagens type I and X. In addition, the cartilaginous matrix, which demonstrated strong staining for s-GAGs and type II collagen, remained in the center of the organoids even after culture in osteogenic media containing BMP2, for a total of 73 days in 3D culture. Our results provide further support of the long-term chondrogenic potential of iPSCs compared to MSCs, which tend to express higher levels of collagen types I and X and undergo hypertrophy relatively quickly, preventing stable cartilage formation.[41–44]

In addition, our organoid was created through a timed delivery of growth factors, whereas many previous MSC-derived osteochondral organoids have been created using different scaffold properties, creating a complex bioreactor, or by mixing MSCs with already differentiated cells.[7,11–13] Instead, we recapitulated endochondral ossification through a stepwise exposure of growth factors, namely TGF-β3 and BMP2, which resulted in organoids with a center of cartilaginous tissue and an outer region of bony calcified tissue. A stepwise strategy for bone formation through endochondral ossification has been previously used with ASC-derived chondrogenic pellets that were implanted *in vivo*.[19] Similar to our results, this process resulted in the formation of a cartilaginous pellet with a calcified outer region. It is interesting that we were able to achieve this result with only BMP2 instead of all the factors the pellet would have been exposed to *in vivo*, such as various matrix metalloproteinases, growth factors, and cytokines. The BMP2 induction of endochondral ossification aligns with previous research in development, injury repair, and regeneration in which BMP2 was found to be vital for chondrocyte maturation and to induce a center of endochondral ossification.[45–47] However, unlike our data, the center of the implanted ASC pellets did not retain their cartilage phenotype.

A similar stepwise strategy has been used with MSCs in which a chondrogenic pellet was subsequently cultured in media containing β-glycerophosphate which resulted in a region of bony tissue surrounding a chondrogenic pellet, similar to the data presented here.[37] However, this group found significant type I collagen present in the chondrogenic area of their organoid, which increased over their 35 days of culture. As iPSCs tend to show little or no hypertrophic differentiation under chondrogenic conditions, the chondrogenic area of the organoids in our present study was not positive for type I collagen. Instead, type I collagen was isolated to the bony exterior regions of the organoids in this study. In addition in our study, we found many bone-specific genes to be upregulated at the final time point, postosteogenesis, including *Alpl*, *Bglap*, *Runx2*, *Ibsp*, *Col1a2*, and *Sp7*.

Surprisingly, no differences were detected between the constructs treated with doxycycline compared to the ones not treated with doxycycline, except for the increase in total DNA content. Although doxycycline has been shown to inhibit cell growth in many human cell types, it actually has a slight protective effect in articular cartilage by helping to inhibit cell death and decreasing degradation of cartilage matrix proteins. This effect likely accounts for the small percentage increase in DNA content in pellets that had doxycycline exposure.[48]

Because no differences in osteogenesis between the dox and no dox groups were detected, we were compelled to further study of the potential of these cells to revert to a pluripotent state. The potential for dedifferentiation and tumorigenesis of cells derived from iPSCs poses a large hurdle for clinical use of these cells.[29,49] Our study provides evidence that differentiated iPSCs may be resistant to reinduction of pluripotency while maintained within an ECM. We found that the addition of doxycycline to the media after chondrogenic differentiation did not cause our iPSC chondrocytes within the 3D cartilaginous matrix to revert to a pluripotent state, as evidenced by the lack of expression of pluripotency factors, as well as colony formation and Nanog, Oct4, and SSEA-1 staining. However, when isolated from the matrix, plated in monolayer, and then treated with doxycycline, we showed the development of colony forming units that were positive for these pluripotency markers. Previous research has demonstrated that doxycycline is readily able to diffuse into a cartilage matrix and activate a doxycycline-inducible vector, even in significantly larger engineered constructs,[50,51] suggesting that our findings were not due to a lack of activation of the vector but rather were likely due to altered behavior of the cells due to interactions with the ECM. In addition, had doxycycline induction only been able to induce pluripotency in the outer layers of our pellets due to limited diffusion into the tissue, pluripotent cells would have been detected in the colony pluripotency assay, which were not.

While a number of previous studies have investigated the influence of matrix properties on the differentiation of stem cells and iPSCs, there is little known regarding the influence of a 3D ECM on maintaining cell phenotype and potentially inhibiting pluripotency.[52–55] *In vivo*, tissue-resident stem cells reside in a 3D niche with mechanical and secreted cues that help them maintain pluripotency.[56,57] When the cells leave the niche, they differentiate, losing their stemness. The cells in our study were encapsulated in an articular cartilage-like matrix, which is unlikely to have the characteristics of a stem cell niche present to aid the cells in reverting to a pluripotent state. It is possible that the cells digested from the matrix and plated in monolayer were primed for reversion, as chondrocytes plated in monolayer tend to dedifferentiate, which changes their gene and protein expression and may allow for greater plasticity of the cells.[56–58] Therefore, it may have been the presence of a 3D matrix that maintained cell shape, rather than specific proteins in the matrix, that prevented reversion to a pluripotent state. In addition, while no true stem cell ''niche'' is present in articular cartilage, the superficial surface of articular cartilage does contain a population of chondroprogenitor cells.[59] Unlike the chondrocytes in the middle and deep zones of the cartilage, cells in the superficial zone are flat, similar to cells in monolayer culture. Although it is clear that the chondrogenic 3D matrix prevented de-differentiation of our cells despite externally providing the otherwise necessary and sufficient factors of pluripotency induction, it is unclear whether a specific matrix protein or the mechanical forces provided by the matrix inhibited de-differentiation. Further research will be necessary to answer this question, which could provide additional insights into future clinical utilization of iPSC-derived tissues.

Conclusion

This study provides a strategy for creation of an osteochondral organoid without the need for multiple cell types, scaffolds, or bioreactors. The creation of this novel iPSC-derived osteochondral organoid provides a platform for

studying normal and pathologic interactions between bone and cartilage at the osteochondral junction.[60] An osteochondral organoid system could provide unique opportunities to study the process of endochondral ossification and hypertrophy *in vitro,* as well as basic biologic interactions at the bone–cartilage interface. These constructs were grown from iPSCs, opening the possibility for *in vitro* modeling of the effects of specific genetic variants as risk factors for OA, skeletal dysplasia, or other musculoskeletal diseases, as well as the possibility for testing drugs in a disease-specific or patient-specific manner.[22,61] Furthermore, while creating these osteochondral organoids, we discovered that the 3D cartilaginous matrix in which the cells were encapsulated prevented reinduction of pluripotency in the cells, a critical finding for the future clinical usability of iPSC-derived tissues.

Acknowledgment

The authors thank Dr. William Horton of Portland Shriners Research Center for providing the COL2-GFP construct.

Disclosure Statement

F.G. is a paid employee of Cytex Therapeutics.

Funding Information

This work was supported by the Shriners Hospitals for Children, the Arthritis Foundation, NIH grants AG15768, AG46927, AR073752, AR072999, AR074992, T32 GM007171 (to S.K.O.), F31AR68217 (to S.K.O), T32 EB018266 (to D.B.K.), the James S. McKelvey Research Scholars Program (to L.G.), and the Nancy Taylor Foundation for Chronic Diseases.

References

1. Lawrence, R.C., Felson, D.T., Helmick, C.G., *et al.* Estimates of the prevalence of arthritis and other rheumatic conditions in the United States. Part, I.I. Arthritis Rheum **58,** 26, 2008.
2. Lories, R.J., and Luyten, F.P. The bone-cartilage unit in osteoarthritis. Nat Rev Rheumatol **7,** 43, 2011.
3. Loeser, R.F., Goldring, S.R., Scanzello, C.R., and Goldring, M.B. Osteoarthritis: a disease of the joint as an organ. Arthritis Rheum **64,** 1697, 2012.
4. Goldring, S.R., and Goldring, M.B. Changes in the osteochondral unit during osteoarthritis: structure, function and cartilage-bone crosstalk. Nat Rev Rheumatol **12,** 632, 2016.
5. Yuan, X.L., Meng, H.Y., Wang, Y.C., *et al.* Bone-cartilage interface crosstalk in osteoarthritis: potential pathways and future therapeutic strategies. Osteoarthritis Cartilage **22,** 1077, 2014.
6. Findlay, D.M., and Kuliwaba, J.S. Bone-cartilage crosstalk: a conversation for understanding osteoarthritis. Bone Res **4,** 16028, 2016.
7. Martin, I., Miot, S., Barbero, A., Jakob, M., and Wendt, D. Osteochondral tissue engineering. J Biomech **40,** 750, 2007.
8. Hu, J.L., Todhunter, M.E., LaBarge, M.A., and Gartner, Z.J. Opportunities for organoids as new models of aging. J Cell Biol **217,** 39, 2018.
9. Fatehullah, A., Tan, S.H., and Barker, N. Organoids as an in vitro model of human development and disease. Nat Cell Biol **18,** 246, 2016.
10. Clevers, H. Modeling development and disease with organoids. Cell **165,** 1586, 2016.
11. Nukavarapu, S.P., and Dorcemus, D.L. Osteochondral tissue engineering: current strategies and challenges. Biotechnol Adv **31,** 706, 2013.
12. Alexander, P.G., Gottardi, R., Lin, H., Lozito, T.P., and Tuan, R.S. Three-dimensional osteogenic and chondrogenic systems to model osteochondral physiology and degenerative joint diseases. Exp Biol Med (Maywood) **239,** 1080, 2014.
13. Lozito, T.P., Alexander, P.G., Lin, H., Gottardi, R., Cheng, A.W., and Tuan, R.S. Three-dimensional osteochondral microtissue to model pathogenesis of osteoarthritis. Stem Cell Res Ther **4 Suppl 1,** S6, 2013.
14. Lin, Z., Li, Z., Li, E.N., *et al.* Osteochondral tissue chip derived from iPSCs: modeling OA pathologies and testing drugs. Front Bioeng Biotechnol **7,** 411, 2019.
15. Mackie, E.J., Ahmed, Y.A., Tatarczuch, L., Chen, K.S., and Mirams, M. Endochondral ossification: how cartilage is converted into bone in the developing skeleton. Int J Biochem Cell Biol **40,** 46, 2008.
16. Mackie, E.J., Tatarczuch, L., and Mirams, M. The skeleton: a multi-functional complex organ: the growth plate chondrocyte and endochondral ossification. J Endocrinol **211,** 109, 2011.
17. Yang, L., Tsang, K.Y., Tang, H.C., Chan, D., and Cheah, K.S. Hypertrophic chondrocytes can become osteoblasts and osteocytes in endochondral bone formation. Proc Natl Acad Sci U S A **111,** 12097, 2014.
18. Hu, D.P., Ferro, F., Yang, F., *et al.* Cartilage to bone transformation during fracture healing is coordinated by the invading vasculature and induction of the core pluripotency genes. Development **144,** 221, 2017.
19. Osinga, R., Di Maggio, N., Todorov, A., *et al.* Generation of a bone organ by human adipose-derived stromal cells through endochondral ossification. Stem Cells Transl Med **5,** 1090, 2016.
20. Scotti, C., Piccinini, E., Takizawa, H., *et al.* Engineering of a functional bone organ through endochondral ossification. Proc Natl Acad Sci U S A **110,** 3997, 2013.
21. Takahashi, K., and Yamanaka, S. Induction of pluripotent stem cells from mouse embryonic and adult fibroblast cultures by defined factors. Cell **126,** 663, 2006.
22. Tiscornia, G., Vivas, E.L., and Izpisua Belmonte, J.C. Diseases in a dish: modeling human genetic disorders using induced pluripotent cells. Nat Med **17,** 1570, 2011.
23. Adkar, S.S., Brunger, J.M., Willard, V.P., Wu, C.L., Gersbach, C.A., and Guilak, F. Genome engineering for personalized arthritis therapeutics. Trends Mol Med **23,** 917, 2017.
24. Elitt, M.S., Barbar, L., and Tesar, P.J. Drug screening for human genetic diseases using iPSC models. Hum Mol Genet **27,** R89, 2018.
25. Diekman, B.O., Christoforou, N., Willard, V.P., *et al.* Cartilage tissue engineering using differentiated and purified induced pluripotent stem cells. Proc Natl Acad Sci U S A **109,** 19172, 2012.
26. Wu, Q., Yang, B., Hu, K., Cao, C., Man, Y., and Wang, P. Deriving osteogenic cells from induced pluripotent stem cells for bone tissue engineering. Tissue Eng Part B Rev **23,** 1, 2017.
27. Limraksasin, P., Kondo, T., Zhang, M., *et al.* In vitro fabrication of hybrid bone/cartilage complex using mouse induced pluripotent stem cells. Int J Mol Sci **21,** 581, 2020.
28. Hamilton, B., Feng, Q., Ye, M., and Welstead, G.G. Generation of induced pluripotent stem cells by reprogramming mouse embryonic fibroblasts with a four transcription fac-

tor, doxycycline inducible lentiviral transduction system. J Vis Exp **33,** 1447, 2009.
29. Medvedev, S.P., Shevchenko, A.I., and Zakian, S.M. Induced Pluripotent Stem Cells: problems and advantages when applying them in regenerative medicine. Acta Naturae **2,** 18, 2010.
30. Itakura, G., Kawabata, S., Ando, M., *et al.* Fail-safe system against potential tumorigenicity after transplantation of iPSC derivatives. Stem Cell Rep **8,** 673, 2017.
31. Mandai, M., Watanabe, A., Kurimoto, Y., *et al.* Autologous induced stem-cell-derived retinal cells for macular degeneration. N Engl J Med **376,** 1038, 2017.
32. Grant, T.D., Cho, J., Ariail, K.S., Weksler, N.B., Smith, R.W., and Horton, W.A. Col2-GFP reporter marks chondrocyte lineage and chondrogenesis during mouse skeletal development. Dev Dyn **218,** 394, 2000.
33. Morris, S.A., Guo, Y., and Zernicka-Goetz, M. Developmental plasticity is bound by pluripotency and the Fgf and Wnt signaling pathways. Cell Rep **2,** 756, 2012.
34. Ying, Q.L., Wray, J., Nichols, J., *et al.* The ground state of embryonic stem cell self-renewal. Nature **453,** 519, 2008.
35. Nichols, J., Silva, J., Roode, M., and Smith, A. Suppression of Erk signalling promotes ground state pluripotency in the mouse embryo. Development **136,** 3215, 2009.
36. Solorio, L.D., Phillips, L.M., McMillan, A., *et al.* Spatially organized differentiation of mesenchymal stem cells within biphasic microparticle-incorporated high cell density osteochondral tissues. Adv Healthc Mater **4,** 2306, 2015.
37. Muraglia, A., Corsi, A., Riminucci, M., *et al.* Formation of a chondro-osseous rudiment in micromass cultures of human bone-marrow stromal cells. J Cell Sci **116,** 2949, 2003.
38. Cui, W., Wang, Q., Chen, G., *et al.* Repair of articular cartilage defects with tissue-engineered osteochondral composites in pigs. J Biosci Bioeng **111,** 493, 2011.
39. Chen, K., Teh, T.K., Ravi, S., Toh, S.L., and Goh, J.C. Osteochondral interface generation by rabbit bone marrow stromal cells and osteoblasts coculture. Tissue Eng Part A **18,** 1902, 2012.
40. Andrade, R., Vasta, S., Pereira, R., *et al.* Knee donor-site morbidity after mosaicplasty - a systematic review. J Exp Orthop **3,** 31, 2016.
41. Pelttari, K., Winter, A., Steck, E., *et al.* Premature induction of hypertrophy during in vitro chondrogenesis of human mesenchymal stem cells correlates with calcification and vascular invasion after ectopic transplantation in SCID mice. Arthritis Rheum **54,** 3254, 2006.
42. Larson, B.L., Yu, S.N., Park, H., *et al.* Chondrogenic, hypertrophic, and osteochondral differentiation of human mesenchymal stem cells on three-dimensionally woven scaffolds. J Tissue Eng Regen Med **13,** 1453, 2019.
43. Occhetta, P., Pigeot, S., Rasponi, M., *et al.* Developmentally inspired programming of adult human mesenchymal stromal cells toward stable chondrogenesis. Proc Natl Acad Sci U S A **115,** 4625, 2018.
44. Diederichs, S., Klampfleuthner FAM, Moradi, B., and Richter, W. Chondral differentiation of induced pluripotent stem cells without progression into the endochondral pathway. Front Cell Dev Biol **7,** 270, 2019.
45. Shu, B., Zhang, M., Xie, R., *et al.* BMP2, but not BMP4, is crucial for chondrocyte proliferation and maturation during endochondral bone development. J Cell Sci **124,** 3428, 2011.
46. Yu, Y.Y., Lieu, S., Lu, C., and Colnot, C. Bone morphogenetic protein 2 stimulates endochondral ossification by regulating periosteal cell fate during bone repair. Bone **47,** 65, 2010.
47. Yu, L., Han, M., Yan, M., Lee, J., and Muneoka, K. BMP2 induces segment-specific skeletal regeneration from digit and limb amputations by establishing a new endochondral ossification center. Dev Biol **372,** 263, 2012.
48. Cylwik, J., Kita, K., Barwijuk-Machala, M., *et al.* The influence of doxycycline on articular cartilage in experimental osteoarthrosis induced by iodoacetate. Folia Morphol (Warsz) **63,** 237, 2004.
49. Liu, Z., Tang, Y., Lu, S., *et al.* The tumourigenicity of iPS cells and their differentiated derivates. J Cell Mol Med **17,** 782, 2013.
50. Glass, K.A., Link, J.M., Brunger, J.M., Moutos, F.T., Gersbach, C.A., and Guilak, F. Tissue-engineered cartilage with inducible and tunable immunomodulatory properties. Biomaterials **35,** 5921, 2014.
51. Rowland, C.R., Glass, K.A., Ettyreddy, A.R., *et al.* Regulation of decellularized tissue remodeling via scaffold-mediated lentiviral delivery in anatomically-shaped osteochondral constructs. Biomaterials **177,** 161, 2018.
52. Lv, H., Li, L., Sun, M., *et al.* Mechanism of regulation of stem cell differentiation by matrix stiffness. Stem Cell Res Ther **6,** 103, 2015.
53. Battista, S., Guarnieri, D., Borselli, C., *et al.* The effect of matrix composition of 3D constructs on embryonic stem cell differentiation. Biomaterials **26,** 6194, 2005.
54. Reilly, G.C., and Engler, A.J. Intrinsic extracellular matrix properties regulate stem cell differentiation. J Biomech **43,** 55, 2010.
55. Zhang, G., Drinnan, C.T., Geuss, L.R., and Suggs, L.J. Vascular differentiation of bone marrow stem cells is directed by a tunable three-dimensional matrix. Acta Biomater **6,** 3395, 2010.
56. Li, L., and Xie, T. Stem cell niche: structure and function. Annu Rev Cell Dev Biol **21,** 605, 2005.
57. Gattazzo, F., Urciuolo, A., and Bonaldo, P. Extracellular matrix: a dynamic microenvironment for stem cell niche. Biochim Biophys Acta **1840,** 2506, 2014.
58. Ma, B., Leijten, J.C., Wu, L., *et al.* Gene expression profiling of dedifferentiated human articular chondrocytes in monolayer culture. Osteoarthritis Cartilage **21,** 599, 2013.
59. Dowthwaite, G.P., Bishop, J.C., Redman, S.N., *et al.* The surface of articular cartilage contains a progenitor cell population. J Cell Sci **117,** 889, 2004.
60. Pan, J., Wang, B., Li, W., *et al.* Elevated cross-talk between subchondral bone and cartilage in osteoarthritic joints. Bone **51,** 212, 2012.
61. Cherry, A.B., and Daley, G.Q. Reprogramming cellular identity for regenerative medicine. Cell **148,** 1110, 2012.

Address correspondence to:
Farshid Guilak, PhD
Center of Regenerative Medicine
Washington University
Couch Biomedical Research Building, Room 3121
Campus Box 8233
Saint Louis, MO 63110
USA

E-mail: guilak@wustl.edu

Received: September 14, 2020
Accepted: October 30, 2020
Online Publication Date: December 21, 2020